BGC 945, a Novel Tumor-Selective Thymidylate Synthase Inhibitor Targeted to α-Folate Receptor–Overexpressing Tumors

David D. Gibbs,[1] Davinder S. Theti,[1] Nadya Wood,[2] Matthew Green,[1] Florence Raynaud,[2] Melanie Valenti,[2] Martin D. Forster,[1] Fraser Mitchell,[1] Vassilios Bavetsias,[2] Elisa Henderson,[2] and Ann L. Jackman[1]

[1]Section of Medicine and [2]Cancer Research UK Centre for Cancer Therapeutics, The Institute of Cancer Research, Sutton, United Kingdom

Abstract

BGC 945 is a cyclopenta[*g*]quinazoline–based, thymidylate synthase inhibitor specifically transported into α-folate receptor (α-FR)–overexpressing tumors. Affinity of BGC 945 for the α-FR is 70% of the high-affinity ligand folic acid. In contrast to conventional antifolates, BGC 945 has low affinity for the widely expressed reduced-folate carrier (RFC). The K_i for isolated thymidylate synthase is 1.2 nmol/L and the IC_{50} for inhibition of the growth of α-FR-negative mouse L1210 or human A431 cells is ~7 μmol/L. In contrast, BGC 945 is highly potent in a range of α-FR-overexpressing human tumor cell lines (IC_{50} ~1-300 nmol/L). Pharmacokinetic variables measured following i.v. injection of 100 mg/kg BGC 945 to KB tumor–bearing mice showed rapid plasma clearance (0.021 L/h) and tissue distribution. The terminal half-lives in plasma, liver, kidney, spleen, and tumor were 2, 0.6, 5, 21, and 28 hours, respectively. Tumor BGC 945 concentration at 24 hours was ~1 nmol/g tissue, at least 10-fold higher than that in plasma or normal tissues. Inhibition of thymidylate synthase in tissues leads to increased incorporation of 5-[^{125}I]-iodo-2′-deoxyuridine ([^{125}I]dUrd) into DNA. Forty-eight hours after injection of 100 mg/kg 6*RS*-BGC 945 ([^{125}I]dUrd injected at 24 hours), tumor was the only tissue with incorporation above control level (6-fold). The RFC-mediated thymidylate synthase inhibitor plevitrexed also increased uptake of [^{125}I]dUrd in tumor (10-fold) but, in contrast, also caused increased incorporation in other normal tissues such as spleen and small bowel (4.5- and 4.6-fold, respectively). These data suggest that BGC 945 selectively inhibits thymidylate synthase in α-FR-overexpressing tumors and should cause minimal toxicity to humans at therapeutic doses. (Cancer Res 2005; 65(24): 11721-8)

Introduction

A novel class of α-folate receptor (α-FR)–targeted thymidylate synthase inhibitors, previously exemplified by CB300638 (BGC 638; Fig. 1), has been discovered that has the potential to be selectively toxic to α-FR-overexpressing tumors compared with normal tissues (1, 2). This is because these agents are selectively transported via receptor-mediated endocytosis into cells via the α-FR. This cell-surface glycoprotein, sometimes referred to as the membrane folate binding protein, is overexpressed in most ovarian cancers (up to 90% of cases) and at various frequencies in many other epithelial tumors (reviewed in refs. 2–4). Normal proliferating tissues such as gut and bone marrow, which are susceptible to thymidylate synthase inhibition, express low levels of the receptor. High levels of α-FR expression are found in placenta, choroid plexus, and kidney tubules. In kidney tubules, the α-FR is located on the apical (luminal) surface and not accessible to blood flow (reviewed in refs. 2–4). This suggests that the normal function of the α-FR in kidney is to salvage folates that have escaped into urine.

Most folate transport occurs via the high-capacity, bidirectional reduced-folate carrier (RFC) system (5–7). The main substrate for the RFC is the circulatory folate 5-methyl tetrahydrofolate. Folic acid (FA) is not a major component of plasma and has very low affinity for the RFC (K_m >100 μmol/L). However, FA has a very high affinity for the α-FR. Expression of the RFC is widespread and, as well as transporting folates, it is a major transporter of antifolate drugs such as methotrexate (MTX), raltitrexed, pemetrexed, and plevitrexed (ZD9331, BGC 9331; refs. 5, 8 and references therein). However, the α-FR, when expressed at very high levels, can function as an additional antifolate transporter although the significance of this is poorly understood and controversial (8–10). The high affinity of FA for the FR has led to the development of new imaging agents and therapies in which FA is conjugated to radionuclides, toxins, cytotoxic drugs, or antibodies (11–14).

In many respects, BGC 638 and its analogues share several properties with plevitrexed. None are metabolized to polyglutamate forms and all are intrinsically very potent inhibitors of thymidylate synthase (BGC 638 K_i = 0.24 nmol/L; plevitrexed K_i = 0.4 nmol/L; refs. 1, 15). These properties are due to the presence of modified glutamate ligands, which in the case of BGC 638 is an L-Glu-γ-D-Glu dipeptide (16, 17). The addition of the second glutamate as the D-enantiomer rather than the L-enantiomer stabilizes antifolates with dipeptide ligands against enzymatic hydrolysis *in vivo* (18, 19). Plevitrexed and BGC 638 display high affinity for the human α-FR (~30% and 53% relative to FA) and can be internalized into tumor cells overexpressing the receptor via the low-capacity α-FR-mediated endocytotic mechanism (1, 8). However, plevitrexed is rapidly transported via the high-capacity RFC (K_m ~1 μmol/L) and is active against both α-FR-positive and α-FR-negative cells (8). In contrast, BGC 638 has low affinity for the RFC (K_m >100 μmol/L) and consequently displays very low cytotoxic activity in α-FR-negative relative to α-FR-expressing cells.

Recently, the synthesis of the 2-hydroxymethyl analogue of BGC 638 (BGC 945; Fig. 1) has been described (20) and we now report a detailed *in vitro* and *in vivo* evaluation of BGC 945. BGC 945 was found to be superior to BGC 638 *in vitro* in terms of its targeting to α-FR-overexpressing tumor cells. Furthermore, it accumulated to

Note: Supplementary data for this article are available at Cancer Research Online (http://cancerres.aacrjournals.org/).

Requests for reprints: Ann L. Jackman, The Institute of Cancer Research, The Haddow Laboratories, 15 Cotswold Road, Sutton, Surrey SM2 5NG, United Kingdom. Phone: 44-208-722-4284; Fax: 44-208-642-7979; E-mail: ann.jackman@icr.ac.uk.

doi:10.1158/0008-5472.CAN-05-2034

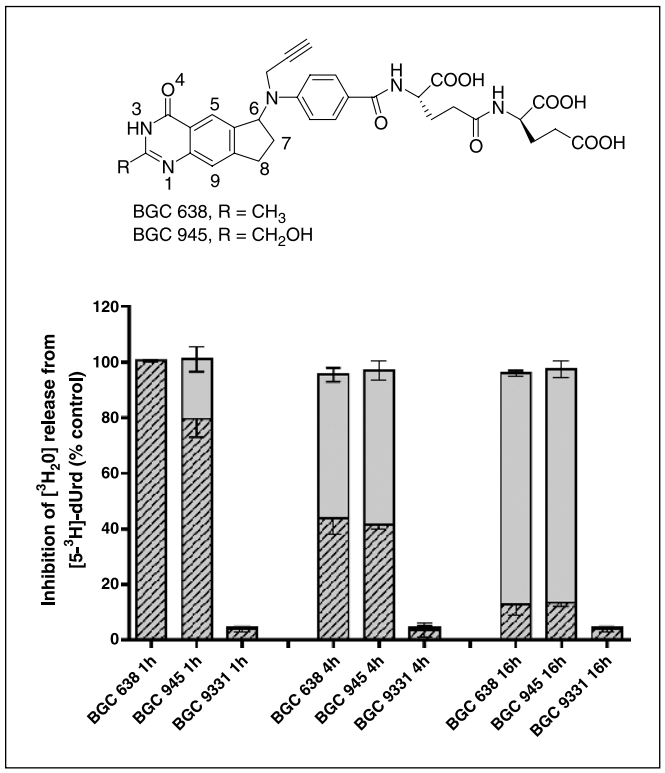

Figure 1. Inhibition of *in situ* thymidylate synthase activity by BGC 945 and BGC 638 in KB cells. Cells were exposed to 30 nmol/L BGC 945 or BGC 638 or 50 nmol/L plevitrexed for 1, 4, and 16 hours. [5-^{3}H]dUrd was then added and the rate of ^{3}H-H_2O release was measured over 1 hour. *Columns,* mean of two independent experiments, expressed as percent control; *hatched area*; bars, range. The activity was also measured in the presence of 1 μmol/L FA to competitively inhibit binding of the compounds to the α-FR (*gray column*); bars, range.

high levels in the KB tumor xenograft relative to normal tissues and selectively inhibited thymidylate synthase in the KB tumor. Based on these data, BGC 945 has been identified as a candidate for phase I clinical study.

Materials and Methods

Compounds. 6*S*-BGC 638, 6*S*-BGC 945, and 6*RS*-BGC 945 were synthesized at the Institute of Cancer Research (17, 20). The 6*S*-BGC 945 used for the *in vitro* JEG-3 experiments and the pharmacokinetic study was a gift of BTG (Fleet Place, London, United Kingdom). Unless stated otherwise, the 6*S*-diastereoisomer of BGC 945, rather than the mixture of 6*RS*-diastereoisomers, was used. Plevitrexed was synthesized at AstraZeneca (Alderley Park, Cheshire, United Kingdom). Compounds were dissolved in 0.15 mol/L $NaHCO_3$ (plus ~1 drop of 1 mol/L NaOH) for *in vitro* use and stored at −20°C as a 10 mmol/L solution for up to 3 months. Dilutions for experiments were made in unsupplemented medium. For *in vivo* use, compounds were dissolved in 0.05 mol/L $NaHCO_3$ and pH adjusted to ~9 by addition of 1 mol/L NaOH.

Inhibition of isolated thymidylate synthase. Partially purified L1210 thymidylate synthase was used to determine the K_i for BGC 945 as previously described (1). The assay was based on a ^{3}H release from [5-^{3}H]dUMP and results were modeled to a tight binding inhibition equation.

Cell culture. A description of the routine culture of A431 (neo-transfected), A431-FBP (transfected with human α-FR), and KB epidermoid cells is published (1). A431 and A431-FBP cell lines were a generous gift from Dr. A. Tomassetti (Instituto Tumori, Milan, Italy). IGROV-1 ovarian carcinoma cells and JEG-3 choriocarcinoma cells [kindly provided by Dr. G. Jansen (Free University, Amsterdam, the Netherlands) and Dr. M. Ratnam (Medical College of Ohio, Toledo, OH), respectively] were cultured in similar conditions to KB cells. Further details can be found in the Supplementary Methods. Mouse L1210, L1210-FBP, and L1210-1565 cell lines were grown as suspension cultures as previously described (9, 15).

Affinity for folate transporters. To estimate affinity for the α-FR, a whole-cell [^{3}H]-FA competitive binding assay, adapted from Westerhof et al. (21), was used (1). Relative affinity is defined as the inverse molar ratio of compound required to inhibit [^{3}H]-FA binding to the surface of L1210-FBP or A431-FBP cells by 50%. The relative affinity of FA is set at 1 (100%). Affinity for the RFC was evaluated by determination of the K_i for inhibition of [^{3}H]MTX (15).

Cell-surface [^{3}H]-folic acid binding capacity. This measures the surface binding of [^{3}H]-FA to cells following brief washing with an acidic saline solution to remove surface bound folates. Details are given by Jansen et al. (22) and modifications by Theti et al. (1).

Growth inhibition studies. We have previously published methods used to evaluate the continuous exposure IC_{50} values for the compounds (the concentration required to inhibit growth by 50% compared with control; ref. 1). The end point was cell viability as measured by an 3-(4,5-dimethylthiazol-2-yl)-2,5-diphenyltetrazolium bromide assay (96-well format) for the A431, A431-FBP, IGROV-1, and JEG-3 cell lines at 72, 96, 96, and 72 hours, respectively, and by cell counting for KB cells (72 hours; 24-well format). The times chosen allowed for ~4 control population doublings. IC_{50} values were also determined in the presence of 1 μmol/L FA, a ligand that competitively inhibits compound binding to the α-FR. This estimates the contribution of other transport mechanisms to the activity of the compounds.

The activity of compounds was also measured in KB cells after different exposure times followed by replacement with compound-free medium (8). Growth inhibition was measured at 72 hours as described above.

The activity of the compounds in JEG-3 cells after 120-hour exposure was measured by counting the number of attached cells. This was done in a T25 tissue culture format and described in the Supplementary Methods.

***In situ* thymidylate synthase assay.** This assay measures the rate of ^{3}H release (as ^{3}H-H_2O) from [5-^{3}H]dUrd over 1 hour and is a semiquantifiable measure of thymidylate synthase inhibition in cultured cells. Details can be found in Theti et al. (1) and is based on the method of Yalowich and Kalman (23). A431-FBP and KB cells were exposed to the thymidylate synthase inhibitors for 1, 4, and 16 hours before the addition of the radiolabeled dUrd.

Mouse studies. Female NCR nude mice were obtained from the ICR breeding colony (6-10 weeks of age). All experiments were conducted in line with the UK Co-ordinating Committee on Cancer Research guidelines for animal welfare (24). Mice were housed (five per box) in filtered air cages and allowed food and water *ad libitum*.

Studies were done with mice fed a folate-free mouse chow (supplied as pellets from TestDiet, Richmond, IL) ~3 weeks before and then during the experiments. Mice have folate levels ~5- to 10-fold higher than humans and, because this may reduce compound binding to the FR, levels are reduced to levels equivalent to those found in humans by administering a folate-free diet (25). The reduction in folate levels was confirmed in our own studies using a Quantaphase II folate radioassay kit (Bio-Rad Labs. Ltd., Hertfordshire, United Kingdom). Plasma folate levels fell from 56 ± 14 to 14 ± 6 nmol/L at 2 to 3 weeks and remained at this level for at least the next 2 weeks (human plasma measured at the same time gave a value of 12 nmol/L).

Cultured KB tumor cells were harvested and resuspended in unsupplemented RPMI medium at 5×10^7 cells/mL and 100 μL were immediately injected s.c. into the flank of host mice. Approximately 14 days later, the tumors in the host mice were ~10 mm in diameter and were excised, cut into 1-mm^3 pieces, and placed s.c. by trochar onto the right flank of mice established on the folate-free mouse chow. Mice remained on this diet until completion of the experiments.

Pharmacokinetics of BGC 945. Mice that had been on the folate-free diet for 5 days were transplanted with tumor and the implants allowed to grow to ~250 mm^3 (19 days after tumor implantation). Samples were taken at 5, 15, 30 minutes and 1, 2, 4, 6, 8, 16, 24, 48, and 72 hours after a single i.v. or i.p. injection of 100 mg/kg BGC 945. Blood was collected and plasma

Table 1. Inhibition of isolated L1210 thymidylate synthase, affinity for α-FR (L1210-FBP cells), and inhibition of L1210 cell lines with different folate transporter expression

	Inhibition of isolated thymidylate synthase K_i (nmol/L)	Affinity for α-FR (% of FA)	Inhibition of cell growth, IC_{50} (nmol/L)			
			L1210 (RFC+/α-FR−)	L1210-1565 (RFC−/α-FR−)	L1210-FBP* (RFC−/α-FR+)	L1210-FBP + 1 μmol/L FA
BGC 945	1.2	70 ± 1.5	7,600	6,400	0.020 ± 0.0047	1,100 ± 690
BGC 638	0.24†	66 ± 8.3†	260 ± 24‡	2,100 ± 310‡	0.40 ± 0.18‡	300 ± 64
BGC 9331	0.4§	54 ± 10‖	24 ± 2.3	1,400 ± 330	0.77 ± 0.21	950 ± 50

NOTE: Results are given as individual results or as mean ± SD ($n \geq 3$).
*L1210-FBP surface [^{3}H]-FA binding capacity = 27 pmol/10^7 cells.
†Also published in Theti et al. (1).
‡Also published in Jackman et al. (2).
§Jackman et al. (15).
‖Theti and Jackman (8).

separated as previously described (26). Liver, spleen, kidney, and tumor were washed in sterile PBS, weighed, and snap frozen.

A validated liquid chromatography-tandem mass spectrometry (LC-MS/MS) method is published for the measurement of BGC 945 in mouse plasma (26). The lower limit for quantification is 25 pmol/mL. This was adapted for the measurement of compound in tissues (see Supplementary Methods).

Biodistribution of 5-[^{125}I]-iodo-2′-deoxyuridine as a pharmacodynamic marker of thymidylate synthase inhibition. 5-[^{125}I]-Iodo-2′-deoxyuridine ([^{125}I]dUrd) is a thymidine analogue that can become incorporated into DNA. The rationale for the development of this method is described later but, briefly, the method exploits the increased thymidine kinase activity when thymidylate synthase is inhibited.

Mice were fed the folate-free diet for 14 days and then transplanted with KB tumor, which were allowed to grow to ~250 mm^3 (~7-10 days after tumor implantation). Groups of three mice were injected i.p. with 1, 10, or 100 mg/kg plevitrexed, BGC 945, BGC 638 or vehicle (0.05 mol/L $NaHCO_3$). Twenty-four hours later, 250 kBq of [^{125}I]dUrd were administered by i.v. injection to the tail vein. The specific activity of the injection solution was ~74 TBq/mmol (37 MBq/mL or 1 mCi/mL). Twenty four hours later, mice were sacrificed and tissues removed as described above for gamma counting. The activity in each tissue was expressed as percent recovery of injected dose. This was calculated by normalizing the activity in each tissue to the wet weight and expressing it as a percentage of the total dose of [^{125}I]dUrd administered. Percent recovery of injected dose ranged from 0.05% in blood to 2.3% in large bowel. Uptake in control plasma after 24 hours was ~5,000 cpm.

Results

Inhibition of isolated L1210 thymidylate synthase. BGC 945 inhibited thymidylate synthase with a K_i of 1.2 nmol/L (Table 1). This was determined by measuring the K_{iapp} at increasing concentrations of the folate cosubstrate. Although a competitive pattern was observed at low substrate concentrations, the mechanism was determined as mixed noncompetitive in common with BGC 638 and several other folate-based thymidylate synthase inhibitors (1). Binding to thymidylate synthase was 5-fold weaker than BGC 638.

Relative affinity for the α-folate receptor. FA has a very high affinity for the α-FR (K_d 0.1-1 nmol/L; ref. 27). In the [^{3}H]-FA competitive binding assay, BGC 945 displayed a slightly lower affinity than FA, ~70% for both mouse L1210-FBP and human A431-FBP cells (Table 1 and data not shown). These are similar to the results for BGC 638.

Affinity for the reduced-folate carrier. The affinity of this class of compound for the RFC is very low and difficult to determine. We have reported the K_i (inhibition of [^{3}H]MTX transport) for BGC 638 as 115 ± 12 and 393 ± 231 μmol/L for human W1L2 and mouse L1210 RFC, respectively, (1). Only 6*RS*-BGC 945 has been evaluated in these cells, giving values of ~2,000 μmol/L (data not shown). For comparison, the K_i values for 6*RS*-BGC 638 were 280 ± 150 and 390 ± 230 μmol/L. This shows a lower affinity of BGC 945 for both mouse and human RFC compared with BGC 638.

Growth inhibition in mouse L1210, L1210-1565, and L1210-FBP cells. Commercial tissue culture media contain supraphysiologic concentrations of FA (2-8 μmol/L) and, as a result, RFC-positive L1210 cells have a down-regulated α-FR (21). Under these conditions, the BGC 945 IC_{50} for L1210 growth inhibition (7.6 μmol/L) was ~30-fold higher than the BGC 638 IC_{50}, and this may be attributable to the lower affinity of BGC 945 for the RFC and isolated thymidylate synthase (Table 1). L1210-1565 cells have a nonfunctional RFC but can survive in the FA-rich media, taking up the vitamin via non-RFC mechanisms. These cells do not express significant levels of the α-FR[3] and are ~3-fold less sensitive to BGC 945 than BGC 638. However, both cell lines are equally sensitive to BGC 945 (IC_{50} ~7 μmol/L) suggesting that neither the RFC or the α-FR are transport routes for this compound in L1210 cells. In contrast, the IC_{50} of BGC 638 for L1210 cells is ~8-fold lower than that for L1210-1565 cells, implying that some RFC-mediated uptake may be occurring in L1210 cells. This is consistent with its higher affinity for the RFC than BGC 945. Nevertheless, uptake of both compounds in L1210 cells is very inefficient with IC_{50} for inhibition of cell growth being 1,100- and 6,000-fold higher than the thymidylate synthase K_i for BGC 638 and BGC 945, respectively. This compares with 60-fold for plevitrexed (K_i RFC = 2 μmol/L; ref. 15). RFC-negative L1210-FBP cells overexpress the α-FR and are remarkably sensitive to BGC 945 (IC_{50} = 0.02 nmol/L), implying that these cells transport it via the α-FR. Furthermore, the IC_{50} for L1210-FBP cells is 1.1 μmol/L in

[3] Unpublished data.

the presence of 1 μmol/L FA that competitively inhibits BGC 945 binding to the α-FR. Interestingly, L1210-FBP cells are 20-fold more sensitive to BGC 945 than BGC 638 in spite of BGC 945 being a 5-fold weaker inhibitor of isolated thymidylate synthase. This suggests that BGC 945 may be transported more efficiently than BGC 638 in L1210-FBP cells and supporting data are given below.

Growth Inhibition in human cell lines. All cell lines used express the RFC and were grown in FA-free media supplemented with 20 nmol/L LV (a physiologic concentration of folate). A431 cells are α-FR negative and are sensitive to folate-based thymidylate synthase inhibitors such as raltitrexed, pemetrexed, and plevitrexed (IC_{50} = 3.1, 40, and 86 nmol/L, respectively; ref. 1). In comparison, the IC_{50} for BGC 945 was 2 to 3 orders of magnitude higher at 6.6 μmol/L (Table 2). This was also 8-fold higher than the IC_{50} for BGC 638, consistent with BGC 945 being 5-fold weaker as an inhibitor of isolated thymidylate synthase. However, the IC_{50} of both compounds for A431-FBP cells were similar at 1.1 and 2.8 nmol/L, respectively. The coaddition of 1 μmol/L FA to A431-FBP cells increased the IC_{50} of BGC 945 and BGC 638 to 6.9 and 0.49 μmol/L, respectively. This order of magnitude increase in the selective advantage of BGC 945 over BGC 638 for α-FR-mediated uptake again suggests a difference in their efficiencies for α-FR-mediated uptake.

The KB epidermoid tumor cell line is often used to evaluate α-FR-targeted strategies because of its constitutively expressed α-FR. KB cells have a surface [^{3}H]-FA binding capacity of 91 pmol/10^7 cells in 20 nmol/L folate (A431-FBP = 171 pmol/10^7 cells) using a [^{3}H]-FA binding assay (1). KB cells were highly sensitive to BGC 945 (IC_{50} = 3 nmol/L) and sensitivity was reduced ~1,500-fold in the presence of 1 μmol/L FA (Table 2). This selectivity for α-FR-mediated uptake was an order of magnitude higher than that for BGC 638.

The IC_{50} for BGC 945 was determined after shorter exposure periods, 1, 4, 8, 24, and 48 hours. The IC_{50} were >100, 20, 3, 0.8, and 0.003 μmol/L, respectively, and approximately the same as seen with BGC 638 (data not shown). In the presence of 1 μmol/L FA, the BGC 945 IC_{50} were >100, 100, <100, 30, and 8 μmol/L, respectively. These latter values were ~10-fold higher than seen with BGC 638 showing that the selective advantage of BGC 945 occurs at all exposure times.

The activity of BGC 945 was evaluated in two cell lines that we determined to express lower levels of the α-FR as measured by their [^{3}H]-FA surface binding capacity (Table 2). IGROV-1 is a human ovarian tumor cell line that binds 23 pmol FA/10^7 cells (~25% of KB) and is less sensitive than KB cells to BGC 945 (IC_{50} = 0.09 μmol/L; Table 2). Importantly, α-FR-mediated uptake is implied by the 41-fold higher IC_{50} in the presence of 1 μmol/L FA. Once again, BGC 638 was less selective for α-FR-mediated uptake (13-fold) largely because of its higher potency than BGC 945 in the presence of FA. The JEG-3 choriocarcinoma cell line displayed a low surface [^{3}H]-FA binding capacity (3.1 pmol/10^7 cells; ~3% of KB cells) and was relatively insensitive to BGC 945 (IC_{50} = 0.32 μmol/L). The IC_{50} increased 6-fold in the presence of FA but this relatively low selectivity for α-FR-mediated uptake over other mechanisms is nonetheless greater than that seen for plevitrexed or BGC 638 (Table 2).

Uptake of BGC 638 and BGC 945 in KB cells. We compared the intracellular concentration of BGC 945 and BGC 638 in KB cells using the same LC-MS/MS method described for the pharmacokinetic measurements (26). A 1-minute wash in acidic buffer (pH 3.5) was used to remove surface-bound compounds (1) following exposure of KB cells to 30 nmol/L compound for 24 hours (~10× continuous exposure IC_{50}). The intracellular levels were 0.068 nmol/mg protein for both compounds (mean of at least two independent experiments; data not shown). In previous work, we showed that the intracellular and total cell-associated concentrations of BGC 638 under the same conditions were ~1 and 6 μmol/L, respectively, (28). Even following a 1-hour incubation with 30 nmol/L BGC 638, the values were ~0.5 and 3.2 μmol/L, respectively, although thymidylate synthase was not inhibited until later. To better evaluate the efficiency of BGC 945 and BGC 638 trafficking through the endosomal apparatus, we used an *in situ* thymidylate synthase assay as a surrogate marker of compound partitioning into the cytosol in tumor cells.

***In situ* thymidylate synthase assay.** KB cells were exposed to 50 nmol/L plevitrexed for 1, 4, and 16 hours (~10× continuous exposure IC_{50}) and thymidylate synthase activity measured. This was <5% of control at all time points and was unaffected by coincubation with 1 μmol/L FA, consistent with rapid RFC-mediated activity of plevitrexed at this concentration. In contrast, thymidylate synthase activity was inhibited more slowly with an equitoxic concentration of BGC 638 or BGC 945 (30 nmol/L) giving values at 1 hour of 100% and 80% of control, respectively (Fig. 1). This decreased to ~45% and ~10% of control for both compounds at 4 and 16 hours, respectively, but was at control level when 1 μmol/L FA was added. Very similar data were obtained

Table 2. Inhibition of the growth of human tumor cell lines with different α-FR expression levels

	α-FR (pmol/10^7 cells)*	BGC 638 IC_{50} (μmol/L)		BGC 945 IC_{50} (μmol/L)		BGC 9331 IC_{50} (μmol/L)	
		−	+	−	+	−	+
A431	<1	0.81 ± 0.36†	0.97 ± 0.58 (1)†	6.6 ± 0.28	6.3 ± 1.3 (1)	0.086 ± 0.036‡	0.067 ± 0.029 (1)‡
A431-FBP	171 ± 42†	0.0028 ± 0.0020†	0.49 ± 0.17 (180)†	0.0011 ± 0.00006	6.9 ± 1.4 (6300)	0.016 ± 0.0097‡	0.034 ± 0.0087 (2)‡
KB	91 ± 17†	0.0036 ± 0.0015†	0.39 ± 0.18 (110)†	0.0033 ± 0.00088	4.8 ± 0.75 (1500)	0.0036 ± 0.0022‡	0.011 ± 0.003 (3)
IGROV-1	23 ± 1.5	0.070 ± 0.024	0.93 ± 0.095 (13)	0.090 ± 0.012	3.7 ± 1.1 (41)	0.053 ± 0.018	0.063 ± 0.01 (1)
JEG-3	3.1 ± 2.9	0.26 ± 0.10	0.61 ± 0.14 (2.3)	0.32 ± 0.23	1.9 ± 0.33 (6)	0.045 ± 0.015	0.063 ± 0.015 (1.5)

NOTE: Results are given as mean ± SD ($n \geq 3$). Values in parentheses refer to the ratio of the IC_{50} + 1 μmol/L FA to the IC_{50} without FA.
*[^{3}H]-FA binding capacity.
†Also published in Theti et al. (1).
‡Also published in Theti and Jackman (8).

in A431-FBP cells (data not shown). Thus, although BGC 945 inhibits thymidylate synthase more slowly than plevitrexed, it is at least as fast as BGC 638 despite its 5-fold weaker inhibition of isolated thymidylate synthase, and supports the hypothesis that BGC 945 is more efficiently trafficked than BGC 638 into the cytosol. A similar study was conducted in L1210-FBP cells exposed to 3 nmol/L of the compounds. Thymidylate synthase activity was 48% and 11% of control at 4 hours for 6*RS*-BGC 638 and 6*RS*-BGC 945, respectively (data not shown) and control levels were observed when 1 μmol/L FA was also added. These data show more rapid α-FR-mediated thymidylate synthase inhibition by BGC 945, which is consistent with its higher L1210-FBP growth inhibitory activity compared with BGC 638.

KB cells were exposed to 30 nmol/L BGC 945 for 1 hour (thymidylate synthase activity 84% of control) before replacement of the medium with compound-free medium and incubation for a further 4 hours. In contrast to what might be expected from a nonpolyglutamatable thymidylate synthase inhibitor, this resulted in a decrease in thymidylate synthase activity (to 55% of control; data not shown). This is consistent with the hypothesis that release of compound from endosomes, rather than endosomal loading, is rate-limiting for induction of thymidylate synthase inhibition.

Effect of exposure time on inhibition of growth and induction of apoptosis in JEG-3 cells. Previous studies with BGC 638 in KB cells showed that it induced thymidylate synthase inhibition, cell cycle arrest in S phase, and growth inhibition several hours later than an equitoxic concentration of plevitrexed (10 × 72 hours IC_{50}; ref. 29). Approximately 50% of total cells were detached and displaying apoptotic morphology at 96 and 48 hours for BGC 638 and plevitrexed, respectively. We therefore argued that these delayed α-FR-mediated effects would be observed even later in JEG-3 cells because of their lower α-FR expression. The sensitivity of JEG-3 cells to 0.03, 0.2, and 1 μmol/L BGC 945 and BGC 638 was evaluated at 120 hours by counting the number of attached cells. In this format, near-exponential growth was maintained in the control flasks for 120 hours (~5 population doublings). The relative contribution of α-FR versus non-α-FR-mediated uptake to the compound activity was evaluated by the coaddition of 1 μmol/L FA. Interestingly, as low as 0.03 μmol/L of both compounds reduced the number of attached cells by slightly more than 50% compared with controls at 120 hours (Fig. 2). Approximately 90% reduction was observed after exposure to 0.2 μmol/L (Fig. 2) and, indeed, ~50% of total cells (attached and detached) were detached and displayed apoptotic morphology (data not shown). These effects were completely prevented by the coaddition of FA. Very few attached cells remained after exposure to 1 μmol/L BGC 945 or BGC 638; furthermore, ~90% of the total cells were detached and apoptotic. However, FA only prevented the cytotoxicity of BGC 945. These data show that increasing the length of exposure of JEG-3 cells to BGC 945 (up to at least 1 μmol/L) beyond the standard 72 hours increases their sensitivity to BGC 945 through an α-FR-mediated mechanism without increasing non-α-FR-mediated effects.

Plasma pharmacokinetics and tissue distribution of BGC 945 in KB tumor–bearing mice. A validated LC-MS/MS method for BGC 945 measurement in plasma was used to evaluate the tissue distribution of the compound in KB tumor–bearing mice. Following i.v. administration, the compound cleared rapidly from plasma (0.021 L/h) as a result of rapid distribution to all tissues (Fig. 3). Maximum tissue concentrations were reached by 5 minutes. The area under the curve $(AUC)_{0-\infty}$ was highest in the liver (665 pmol/g h) and lowest in the spleen (33 pmol/g h). Tumor

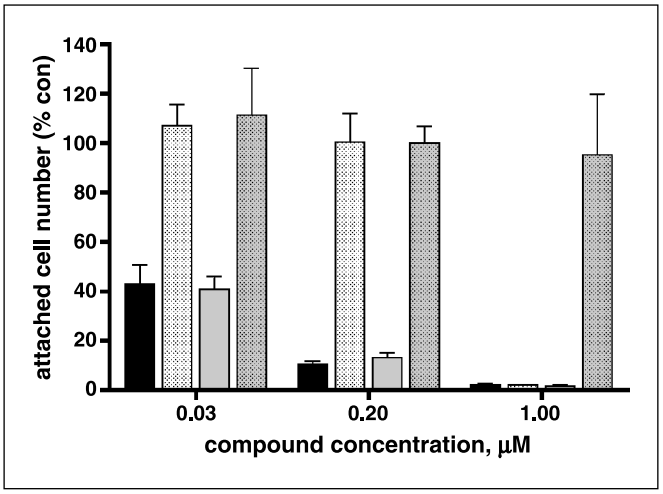

Figure 2. Effect of BGC 945 and BGC 638 on the growth of JEG-3 cells. JEG-3 cells (1×10^5) were exposed to 0.03, 0.2, and 1 μmol/L BGC 638 (*black columns*) or BGC 945 (*gray columns*) and the cells remaining attached to the plastic flasks were collected and counted at 120 hours. In parallel, cells were coincubated with compound and 1 μmol/L FA to competitively and selectively inhibit compound binding to the α-FR (*stippled*). *Columns,* mean of three or four independent experiments; *bars,* SE.

AUC was 117 pmol/g h (see Supplementary Table S3). The apparent volume of distribution was high in the tumor (1.1 L) with a moderate clearance (0.026 L/h) and, as a consequence, BGC 945 in the tumor had a longer half-life (28 hours) compared with other tissues. The volume of distribution was also high in the spleen (2.8 L) and levels remained above the limit of quantification (25 pmol/g) for up to 72 hours, resulting in a long half-life (21 hours). The terminal half-life in plasma was 2 hours and levels were only detectable for up to 16 hours. The terminal half-lives for liver and kidney (1 and 5 hours, respectively) were also short and levels fell below the limit of quantification by 8 and 24 hours, respectively. The tumor level at 24 hours was ~1 nmol/g tissue (~1 μmol/L; i.e., >40-fold higher than plasma or liver and ~10-fold higher than kidney and spleen). At 72 hours, tumor levels exceeded the kidney and spleen concentration by ~40- and ~13-fold, respectively.

After i.p. injection, BGC 945 was well absorbed from the peritoneal cavity (Fig. 3; Supplementary Table S3). The plasma AUC was ~50% higher for i.p. compared with i.v. administration and was also higher in spleen, kidney, and liver by this route. Tumor AUC was similar via either route.

The effect of BGC 638, BGC 945, and BGC 9331 on the biodistribution of 5-[^{125}I]-iodo-2′-deoxyuridine in KB tumor–bearing mice. [^{125}I]dUrd enters cells and is phosphorylated by thymidine kinase to [^{125}I]5-IdUMP and, after further phosphorylation to the triphosphate, is incorporated into DNA. [^{125}I]dUrd is unstable and is extensively metabolized (30); nevertheless, several studies have shown that radiolabeled IdUrd can be used as an imaging agent to estimate cell proliferation (31). Thymidylate synthase inhibition increases the flux through thymidine kinase (32). Hence, thymidylate synthase inhibition increases the pool of [^{125}I]dUTP available for incorporation into DNA both by increasing flux through thymidine kinase and reducing deiodination by thymidylate synthase. For example, uptake of [^{125}I]dUrd into mouse mammary carcinoma cells is increased by treatment with both MTX and 5-fluorouracil (33) and 5-fluorodeoxyuridine increases [^{125}I]dUrd uptake by glioblastoma xenografts (31).

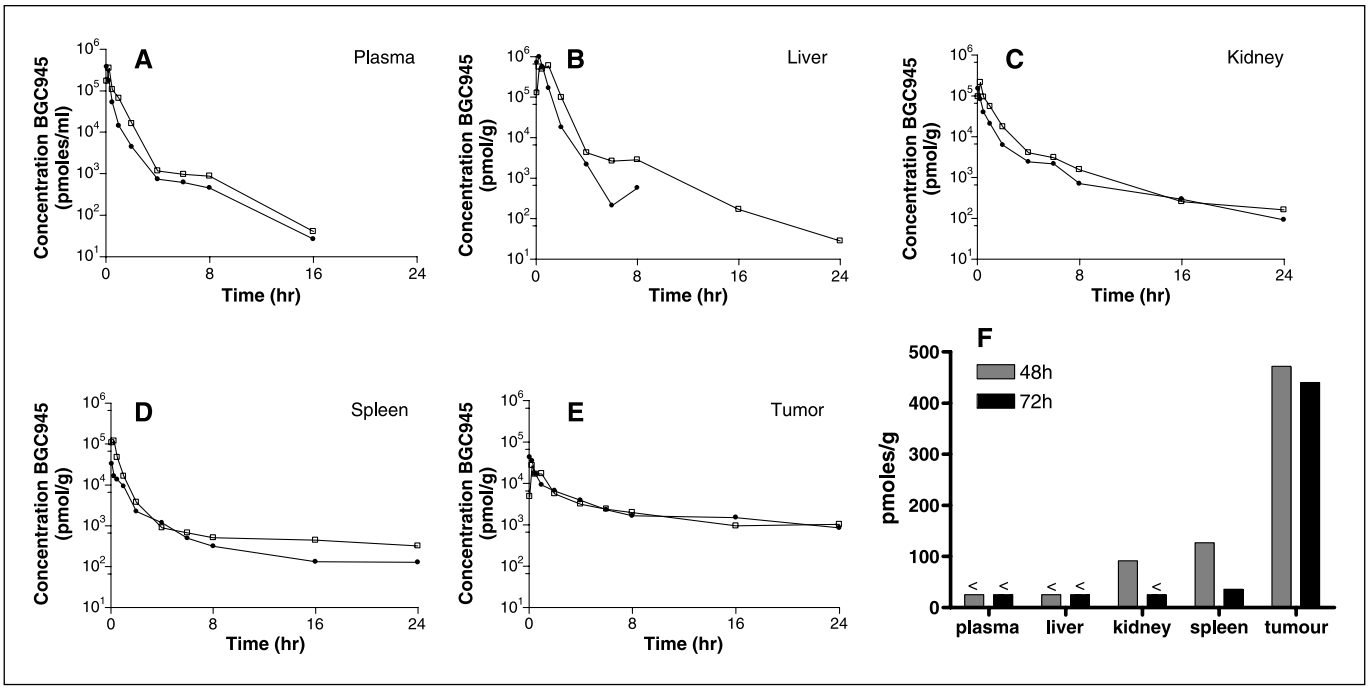

Figure 3. Plasma and tissue concentration of BGC 945 in KB tumor–bearing mice. KB tumor–bearing mice were injected with 100 mg/kg BGC 945 by either i.v. or i.p. administration. Plasma and tissues were collected at the times indicated. *A* to *E*, 0 to 24 hour concentration versus time curves. *Points* and *columns,* mean of three mice. ●, i.v. data; □, i.p. data. The limit of quantification was 25 pmol/mL (g). At later time points, BGC 945 could still be detected in the kidney, spleen, and tumor and the i.v. results are given in (*F*).

The effect of administration of the thymidylate synthase inhibitors on the biodistribution of [^{125}I]dUrd was studied in mice bearing KB xenografts. At 1, 4, 6, and 24 hours after i.p. injection of solvent or 100 mg/kg plevitrexed, 250 kBq of [^{125}I]dUrd were injected i.v. and the tissues were removed for gamma counting 24 hours later. In the solvent controls the radioactivity in the tissues (expressed as percent of total dose of [^{125}I]dUrd administered) ranged from 0.05% in liver to 2.3% in large bowel (liver = blood < kidney < stomach < tumor < spleen < small bowel < large bowel; data not shown). Increased uptake relative to control was observed in spleen, KB xenograft, small bowel, large bowel, kidney, and liver at similar levels at all time points. The results of three independent experiments done at the 24-hour time point showed that the method was reproducible. The highest increase was in tumor (1,020 $\pm$ 120%), followed by spleen (457 $\pm$ 158%), small bowel (462 $\pm$ 25%) and large bowel (338%; $P < 0.05$ for all these results). For other tissues, the increases were as follows: large bowel, 338 $\pm$ 195%; stomach, 221 $\pm$ 51%; blood, 219 $\pm$ 46%; kidney, 184 $\pm$ 39%; and liver, 173 $\pm$ 32%.

In two experiments, treatment with plevitrexed was compared with BGC 638 and 6*RS*-BGC 945. The 6*S*-BGC 945 was not available for these experiments. However, in cell culture, 6*RS*-BGC 945 consistently gave IC_{50} values that were between 50% and 100% of those of the 6*S*-BGC 945 (data not shown). Furthermore, 6*RS*-BGC 945 was ~2-fold less active than 6*S*-BGC 945 in the *in situ* thymidylate synthase inhibition assay. In contrast with the effects of plevitrexed on several tissues, the α-FR-targeted compounds only increased incorporation in the tumor (Fig. 4). In one of the experiments, the effect of reducing the doses was evaluated. Treatment with 10 mg/kg plevitrexed increased uptake in tumor (6.5-fold) and small bowel (5-fold) and although values were increased in spleen, stomach, and large bowel (1.5- to 2-fold), the differences were not significantly different from control (data not shown). After treatment with 1 mg/kg plevitrexed, uptake was higher than control in small bowel and stomach (statistically significant only in small bowel) but not in other tissues. Treatment with BGC 638 and 6*RS*-BGC 945 at a dose of 10 mg/kg showed some increase in uptake (2- to 4-fold) in tumor but the difference did not attain statistical significance. No effect was observed at 1 mg/kg.

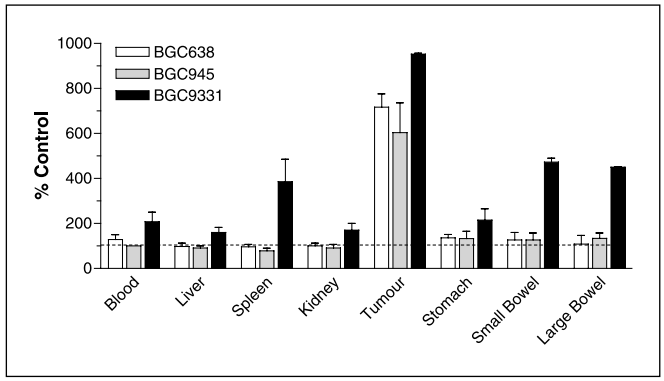

Figure 4. The biodistribution of [^{125}I]dUrd as a pharmacodynamic marker of thymidylate synthase inhibition in KB tumor–bearing mice. [^{125}I]dUrd is a thymidine analogue that can be incorporated into DNA through the activity of thymidine kinase. Thymidylate synthase inhibition leads to increased utilization of the thymidine kinase salvage pathway and consequently increased incorporation of radiolabeled IdUrd into the DNA of tissues. Mice were injected i.p. with 100 mg/kg BGC 9331, BGC 638, or 6*RS*-BGC 945 and 250 kBq of [^{125}I]dUrd i.v. 24 hours later. The tissues were removed for gamma counting 24 hours later. *Columns,* mean uptake in treated mice relative to controls from two independent experiments; *bars,* range.

Discussion

Thymidylate synthase inhibitors are active anticancer agents but their usefulness is limited by toxicity in normal proliferating tissues such as bone marrow and gut. Our challenge was to develop a tumor-targeted thymidylate synthase inhibitor, and the strategy we adopted was to exploit the overexpression of the α-FR in some epithelial tumors. It was essential that the new agent should not only bind to the α-FR but should also be efficiently transported by receptor-mediated endocytosis and unloaded into the cytoplasm, rather than being recycled with the receptor back to the cell surface. It was also essential that the agent was poorly transported by the ubiquitously expressed RFC. Although we have concentrated on the α-FR targeting aspects, a preliminary account suggests that the β-FR should also be considered as a target for folate-based thymidylate synthase inhibitors (34).

We previously reported that the activity of α-FR-targeted thymidylate synthase inhibitors could not be predicted by α-FR surface binding affinity (2, 29) and is now illustrated by the comparison of BGC 638 and BGC 945. Both compounds displayed similar affinity for the α-FR but BGC 945 was a 5-fold weaker inhibitor of isolated thymidylate synthase. Nevertheless, BGC 945 inhibited thymidylate synthase *in situ* and the growth of α-FR-overexpressing tumor cells at a similar rate and this was ascribed to more efficient trafficking of intracellular BGC 945 out of the endosomal compartments into the cytosol. Further transport studies would be facilitated by the use of a radiolabeled compound and separation of endosomal fractions. The *in situ* thymidylate synthase assay also showed the relatively slow rate with which the agents were trafficked compared with the faster RFC-mediated transport of plevitrexed. Data suggest that release of BGC 945 and BGC 638 from the endosomes is the rate-limiting factor rather than surface binding or transport into the endosomal apparatus.

Receptor-mediated endocytosis is a low-capacity transport mechanism and it is predicted that several rounds of receptor recycling to the cell surface may be required to build up sufficiently high levels of BGC 945 in the cytosol to give an antitumor effect. The number of rounds should be dependent, at least in part, on the number of functional receptors expressed on the cell surface. A relationship was shown between [^{3}H]-FA binding levels in our cell line panel and the sensitivity of the cell lines to BGC 945 or BGC 638 in a 72-hour growth inhibition assay. Nevertheless, α-FR-mediated transport is implied for all the cell lines by the increased IC_{50} in the presence of 1 μmol/L FA, particularly for BGC 945. The smallest increase was observed in JEG-3 cells (6- and 2.3-fold for BGC 945 and BGC 638, respectively), which is consistent with its lowest α-FR expression. This implies that the dose of both compounds, particularly BGC 638, required for inhibition of the growth of a tumor expressing relatively low functional receptor levels *in vivo* may be close to the dose that could have effects on normal tissues. However, because of the predicted slow rate of accumulation of compound in cells expressing low levels of α-FR, we studied the effect of increasing exposure time to a range of BGC 945 concentrations in JEG-3 cells. As little as 0.03 μmol/L of the compounds (~10% of the 72-hour IC_{50}) induced growth arrest and apoptosis at 120 hours and the level increased with increasing concentration. One micromolar of BGC 945 or BGC 638 induced a high level of cytotoxicity but the coaddition of 1 μmol/L FA only prevented BGC 945 cytotoxicity. This suggests that long, continuous exposure to BGC 945 would induce α-FR-mediated antitumor activity *in vivo* even in tumors expressing a relatively low level of α-FR.

The pharmacokinetics of BGC 945 was studied in KB tumor–bearing mice following a dose of 100 mg/kg. Rapid distribution to all tissues was observed. The volume of distribution was highest in tumor compared with normal tissues and the terminal half-life was longest in tumor (28 hours). It was important to determine whether the high initial plasma concentration of BGC 945 could lead to uptake and retention into normal tissues by non-α-FR-mediated mechanisms. However, the concentrations achieved suggest that this does not occur. The plasma concentrations of ~10 and 1 μmol/L at 1 and 4 hours, respectively, were much lower than the IC_{50} of BGC 945 after the same exposures in A431 cells (>30 μmol/L; data not shown) or KB cells protected with FA (>100 μmol/L). The tumor level at 24 hours was ~1 nmol/g (~1 μmol/L) and exceeded that of normal tissues by 10- to >40-fold at 24 hours. The tumor concentration was ~0.5 μmol/L at 72 hours and exceeded the KB IC_{50} (72-hour exposure) by ~150-fold. However, without knowing the distribution of BGC 945 in extracellular matrix, cell surface, and the intracellular compartments, it is difficult to extrapolate from measured concentrations to predict antitumor activity. We therefore required further evidence that the tumor localization observed *in vivo* leads to selective inhibition of thymidylate synthase in tumors.

Antitumor activity and therapeutic index in tumor-bearing mice are the traditional end points in preclinical drug development. However, mice are not very meaningful models for thymidylate synthase inhibitors (15, 35–37) because they have plasma levels of thymidine, a salvage precursor of thymidine nucleotides, ~100-fold higher than humans (38, 39). Repeated dosing of mice with conventional antifolate thymidylate synthase inhibitors leads to a 2- to 3-fold reduction in the circulating thymidine level that we believe is attributable to increased thymidine salvaging when thymidylate synthase is inhibited in normal proliferating tissues (38, 40). This probably explains the antitumor activity, albeit fairly modest, of thymidylate synthase inhibitors in human tumor xenografts (35, 41). In contrast, dosing with BGC 945 was not accompanied by a reduction in plasma thymidine even when 16 daily injections of 100 mg/kg were given to KB tumor–bearing mice (data not shown). This is explained by the tumor targeting of BGC 945. Nevertheless, in this experiment, there was a modest ~5-day tumor growth delay observed (P = 0.085; data not shown). We felt that more meaningful information in mice would be obtained from the measurement of pharmacodynamic end points in tumor and normal tissues. The biodistribution of radioactivity following administration of [^{125}I]dUrd to mice that had received a single 100 mg/kg dose of compound 24 hours earlier was used as a marker of thymidylate synthase inhibition. Plevitrexed induced an increase in the levels of radioactivity in several proliferating tissues, including bowel and tumor, whereas BGC 638 and 6*RS*-BGC 945 inhibited thymidylate synthase selectively in the tumor. Taken together, these results show that BGC 945 not only selectively localizes to the tumor through surface receptor binding but is also efficiently transported into KB tumor *in vivo*.

An increase in plasma dUrd is an established pharmacodynamic end point for thymidylate synthase inhibitors and is a consequence of increased intracellular dUMP following thymidylate synthase inhibition in proliferating tissues (38, 40, 42). Following two daily doses of 100 mg/kg BGC 945, there was no increase in plasma dUrd compared with an ~3-fold increase observed with the same dose

of plevitrexed (ref. 43 and data not shown). Taken together with results presented in this article, it can be concluded that BGC 945, at the dose used, does not inhibit thymidylate synthase in normal proliferating tissues. Furthermore, BGC 945 (100 mg/kg daily for 16 days) did not lead to body weight loss, macroscopic signs of toxicity to the major organs, or a change in renal function (43). These data show that BGC 945 is probably not inducing effects related to its FR binding properties that might be independent of its thymidylate synthase inhibitory role.

In summary, BGC 945 is an α-FR-targeted thymidylate synthase inhibitor that has superior *in vitro* properties to the first member of this drug class, BGC 638. It displays a large concentration window in which α-FR-mediated uptake is probably the only uptake mechanism. Targeting thymidylate synthase inhibitors to tumors by virtue of selective α-FR-mediated transport is feasible in mice bearing α-FR-overexpressing tumors and, as a consequence, BGC 945 has been nominated for clinical development.

Acknowledgments

Received 6/10/2005; revised 9/4/2005; accepted 9/13/2005.

Grant support: Cancer Research United Kingdom, BTG International (F. Mitchell), and Prof. M. Gore for part of a clinical fellowship (D.D. Gibbs).

The costs of publication of this article were defrayed in part by the payment of page charges. This article must therefore be hereby marked *advertisement* in accordance with 18 U.S.C. Section 1734 solely to indicate this fact.

We thank Prof. P. Workman, Prof. S. Kaye, Dr. S. Eccles, and Dr. M. Ormerod for the advice, support, and encouragement given throughout these studies.

References

1. Theti DS, Bavetsias V, Skelton LA, et al. Selective delivery of CB300638, a cyclopenta[*g*]quinazoline-based thymidylate synthase inhibitor into human tumour cell lines overexpressing the α-isoform of the folate receptor. Cancer Res 2003;63:3612–8.
2. Jackman AL, Theti DS, Gibbs DD. Antifolates targeted specifically to the folate receptor. Adv Drug Deliv Rev 2004;56:1111–25.
3. Antony AC. Folate receptors: reflections on a personal odyssey and a perspective on unfolding truth. Adv Drug Deliv Rev 2004;56:1059–66.
4. Elnakat H, Ratnam M. Distribution, functionality and gene regulation of folate receptor isoforms: implications in targeted therapy. Adv Drug Deliv Rev 2004; 56:1067–84.
5. Jansen G. Receptor- and carrier-mediated transport systems for folates and antifolates, In: Jackman AL, editor. Antifolate drugs in cancer chemotherapy. Totowa (NJ): Humana Press, Inc.; 1999. p. 293–21.
6. Antony AC. The biological chemistry of folate receptors. Blood 1992;79:2807–202.
7. Whetstine JR, Flatley RM, Matherly LH. The human reduced folate carrier gene is ubiquitously and differentially expressed in normal human tissues: identification of seven non-coding exons and characterization of a novel promoter. Biochem J 2002;367:629–40.
8. Theti DS, Jackman AL. The role of α-folate receptor-mediated transport in the antitumour activity of antifolate drugs. Clin Cancer Res 2004;10:1080–9.
9. Westerhof GR, Schornagel JH, Kathmann I, et al. Carrier and receptor-mediated transport of folate antagonists targeting folate dependent enzymes: correlates of molecular-structure and biological activity. Mol Pharmacol 1995;48:459–71.
10. Chattopadhyay S, Wang Y, Zhao R, Goldman ID. Lack of impact of loss of constitutive folate receptor α expression, achieved by RNA interference, on the activity of the new generation antifolate pemetrexed in HeLa cells. Cancer Res 2004;10:7986–93.
11. Low PS, Antony AC. Folate receptor-targeted drugs for cancer and inflammatory diseases. Adv Drug Deliv Rev 2004;56:1055–8.
12. Leamon CP, Reddy JA. Folate-targeted chemotherapy. Adv Drug Deliv Rev 2004;56:1127–41.
13. Ke C-Y, Mathias CJ, Green MA. Folate-receptor-targeted radionuclide imaging agents. Adv Drug Deliv Rev 2004;56:1143–60.
14. Lu Y, Sega E, Leamon CP, Low PS. Folate receptor-targeted immunotherapy of cancer: mechanism and therapeutic potential. Adv Drug Deliv Rev 2004;56: 1161–76.
15. Jackman AL, Kimbell R, Aherne GW, et al. The cellular pharmacology and *in vivo* activity of a new anticancer agent, ZD9331: a water-soluble, non-polyglutamatable quinazoline-based inhibitor of thymidylate synthase. Clin Cancer Res 1997;3:911–21.
16. Bavetsias V, Marriott JH, Melin C, et al. Synthesis of cyclopenta[*g*]quinazoline-based antifolates, a novel class of thymidylate synthase inhibitors. J Med Chem 2000;43:1910–26.
17. Bavetsias V, Marriott JH, Theti D, Melin JC, Wilson SC, Jackman AL. Cyclopenta[*g*]quinazoline-based antifolates: the effect of the chirality at the 6-position on the inhibition of thymidylate synthase. Bioorg Med Chem Lett 2001;11:3015–7.
18. Bavetsias V, Jackman AL, Kimbell R, Gibson W, Boyle FT, Bisset GMF. Quinazoline antifolate thymidylate synthase inhibitors: γ-linked L-D, D-D and D-L dipeptide analogues of 2-desamino-2-methyl-N^{10}-propargyl-5,8-dideazafolic acid (ICI 198583). J Med Chem 1996;39:73–85.
19. Jodrell DI, Gibson W, Bissett GMF, Boyle FT, Judson IR, Jackman AL. The *in vivo* metabolic stability of dipeptide analogues of the quinazoline antifolate, ICI 198583, in mice. Biochem Pharmacol 1993;46:2229–34.
20. Henderson EA. Folate receptor targeting: synthetic approaches to nonpolyglutamatable inhibitors of thymidylate synthase. Ph.D. thesis. Faculty of Science. London: University of London; 2001.
21. Westerhof GR, Jansen G, Van Emmerik N, et al. Membrane transport of natural folates and antifolate compounds in murine L1210 leukemia cells: the role of carrier- and receptor-mediated transport systems. Cancer Res 1991;51:5507–13.
22. Jansen G, Westerhof GR, Kathmann I, Rademaker BC, Rijksen G, Schornagel JH. Identification of a membrane-associated folate-binding protein in human leukemic CCRF-CEM cells with transport related methotrexate resistance. Cancer Res 1989;49:2455–9, 1989. (correction in Cancer Res 1995;55: 4203; cell line now designated L1210-FBP.)
23. Yalowich JC, Kalman TI. Rapid determination of thymidylate synthase activity and its inhibition in intact L1210 leukemia cells *in vitro*. Biochem Pharmacol 1985;34:2319–24.
24. Workman P, Twentyman P, Balkwill F, et al. United Kingdom Co-ordinating Committee on Cancer Research (UKCCCR) guidelines for the welfare of animals in experimental neoplasia (second edition). Br J Cancer 1998;77:1–10.
25. Schmitz JC, Grindey GB, Schultz RM, Priest DG. Impact of dietary folic acid on reduced folates in mouse plasma and tissues. Relationship to dideazatetrahydrofolate sensitivity. Biochem Pharmacol 1994;48:319–25.
26. Wood N, Gibbs DD, Jackman AL, Henley A, Workman P, Raynaud F. Validation of a high-performance liquid chromatography tandem mass spectrometry assay for the quantification of BGC 945 and BGC 638 in mouse plasma. J Chromatogr B Analyt Technol Biomed Life Sci 2005;824:181–8.
27. Wang X, Shen F, Freisheim JH, Gentry LE, Ratnam M. Differential stereospecificities and affinities of folate receptor isoforms for folate compounds and antifolates. Biochem Pharmacol 1992;44:1898–01.
28. Gibbs DD. The *in vivo* development of folate receptor targeted thymidylate synthase inhibitors. Ph.D. thesis, Faculty of Medicine, University of London, UK; 2003.
29. Theti DS. Development of a novel class of thymidylate synthase inhibitor targeted to α-folate receptor overexpressing tumours. Ph.D. thesis, Faculty of Science, University of London, UK; 2000.
30. Carreras CW, Santi DV. The catalytic mechanism and structure of thymidylate synthase. Annu Rev Biochem 1995;64:721–62.
31. Dupertuis YM, Vazquez M, Mach JP, et al. Fluorodeoxyuridine improves imaging of human glioblastoma xenografts with radiolabelled iododeoxyuridine. Cancer Res 2001;61:7971–7.
32. Xu Y, Plunkett W. Regulation of thymidine kinase and thymidylate synthase in intact human lymphoblast CCRF-CEM cells. J Biol Chem 1993;268:22363–8.
33. Mester J, DeGoeij K, Sluyser M. Modulation of [5-^{125}I]iododeoxyuridine incorporation into tumour and normal tissue DNA by methotrexate and thymidylate synthase inhibitors. Eur J Cancer 1996;32A:1603–8.
34. Jansen G. Antifolates in chronic inflammatory diseases/rheumatoid arthritis: what can we learn from cancer and vice versa. Pteridines 2005;16:46.
35. Hughes LR, Stephens TC, Boyle FT, Jackman AL. Raltitrexed (Tomudex), a highly polyglutamatable antifolate thymidylate synthase inhibitor: design and preclinical activity. In: Jackman AL, editor. Antifolate drugs in cancer therapy. Totowa (NJ): Humana Press; 1999. p. 147–65.
36. Cao S, McGuire JJ, Rustum YM. Antitumor activity of ZD1694 (tomudex) against human head and neck cancer in nude mouse models: role of dosing schedule and plasma thymidine. Clin Cancer Res 1999;5:1925–34.
37. Teicher BA, Chen V, et al. Treatment regimens including the multitargeted antifolate LY231514 in human tumor xenografts. Clin Cancer Res 2000;6: 1016–23.
38. Jackman AL, Taylor GA, Calvert AH, Harrap KR. Modulation of antimetabolite effects: effects of thymidine on the efficacy of the quinazoline-based thymidylate synthetase inhibitor, CB 3717. Biochem Pharmacol 1984;33:3269–75.
39. Benepal T, Mitchell F, Gibbens I, Gore M, Jackman AL. Estimation of plasma thymidine in healthy volunteers vs. cancer patients by high performance liquid chromatography. Br J Cancer 2003;88:S56.
40. Clarke SI, Farrugia DC, Aherne GW, Pritchard DM, Benstead J, Jackman AL. Balb/c mice as a preclinical model for raltitrexed-induced gastrointestinal toxicity. Clin Cancer Res 2000;6:285–96.
41. Boyle FT, Stephens TC, Averbuch SD, Jackman AL. ZD9331, preclinical and clinical studies. In: Jackman AL, editor. Antifolate drugs in cancer chemotherapy. Totowa (NJ): Humana Press, Inc.; 1999. p. 243–60.
42. Ford HER, Mitchell F, Cunningham D, et al. Patterns of elevation of plasma 2′-deoxyuridine, a surrogate marker of thymidylate synthase inhibition, following administration of different schedules of 5-fluorouracil and the specific thymidylate synthase inhibitors raltitrexed (Tomudex®) and ZD9331. Clin Cancer Res 2002; 8:103–9.
43. Forster MD, Raynaud F, Wood N, et al. CB300945, a new α-folate receptor targeted thymidylate synthase inhibitor. Proc Am Assoc Cancer Res 2004;45:1066.